Quantum theory of the mazer. II. Extensions and experimental considerations

Markus Löffler,[1,2,3] Georg M. Meyer,[1,2,3] Michael Schröder,[2,4] Marlan O. Scully,[1,2] and Herbert Walther[1,3]
[1]*Max-Planck-Institut für Quantenoptik, Hans-Kopfermann-Strasse 1, D-85748 Garching, Germany*
[2]*Department of Physics, Texas A&M University, College Station, Texas 77843*
and Texas Laser Laboratory, Houston Advanced Research Center, The Woodlands, Texas 77381
[3]*Sektion Physik, Ludwig-Maximilians-Universität, München, Germany*
[4]*Abteilung für Quantenphysik, Universität Ulm, D-89069 Ulm, Germany*
(Received 9 April 1997)

The quantum theory of the mazer is extended by giving exact analytical solutions for a smooth potential and comparing them with the mesa potential considered earlier. Furthermore, WKB solutions for sinusoidal mode functions are found, leading to interesting features such as a state-changing or state-preserving mirror for atoms. Experimental parameters are taken into account to show that it is in principle possible to realize the mazer experimentally. [S1050-2947(97)01511-4]

PACS number(s): 42.50.Ar, 32.80.−t, 42.50.Dv, 84.40.Ik

I. INTRODUCTION

It has been shown recently [1,2] that a completely new kind of induced emission occurs when a micromaser is pumped by ultracold atoms. In an ordinary micromaser radiation is amplified via stimulated emission [3,4]. For ultracold atoms the interplay between the quantized center-of-mass (CM) motion and the atom-field interaction leads to microwave amplification via z-motion–induced emission of radiation (mazer). In the preceding paper [2] (hereafter referred to as paper I) the quantum theory of the mazer has been developed. The physical mechanism governing mazer action can be understood in the atom-field dressed-state picture. One of the dressed-state components, say $|\gamma_{n+1}^{-}\rangle$, sees a potential well, as the other one ($|\gamma_{n+1}^{+}\rangle$) sees a potential barrier. In the mazer regime the kinetic energy of the atoms is so small that the component that sees the barrier can be reflected while the other one is transmitted. The emission probability and the photon statistics of the cavity depend on the reflection and transmission coefficients for the dressed-state components. In Ref. [1] and paper I, these coefficients are given analytically for a mesa potential. In the present paper, the problem is solved for a sech^2 potential as well as for sinusoidal potentials.

Our main results are as follows. Also for a smooth sech^2 potential, mazer resonances can be found, as long as the interaction length is not too large. In the intermediate regime between the Rabi limit and the mazer limit the properties of the mazer depend crucially on the form of the potential. The scaling parameters governing this regime are identified. A mazer with a sinusoidal potential can serve as a very interesting device for atom optics, namely, as a state-preserving or state-changing atomic mirror. The most promising setup for an experimental realization of the mazer is a reentrant cavity. With such a device it should be possible to see the mazer resonances experimentally.

This paper is organized as follows: in Sec. II analytical solutions are given both for a mesa mode function and for a sech^2 mode function. The features and differences of the emission probability for the different modes are discussed in Sec. II C. In Sec. III WKB solutions for sinusoidal modes are presented. Finally, experimental parameters are taken into account in Sec. IV and different possible experimental setups are considered.

II. MESA MODE VERSUS sech^2 MODE

The probability for the atoms to emit a photon, if initially the atoms are in the upper state and the cavity contains n photons, is given by [1] (see paper I for details)

$$P_{\text{emission}}(n)=|R_{b,n+1}|^2+|T_{b,n+1}|^2, \tag{1}$$

where

$$R_{an}=\tfrac{1}{2}(\rho_n^{+}+\rho_n^{-}),\quad T_{an}=\tfrac{1}{2}(\tau_n^{+}+\tau_n^{-}),$$
$$R_{b,n+1}=\tfrac{1}{2}(\rho_n^{+}-\rho_n^{-}),\quad T_{b,n+1}=\tfrac{1}{2}(\tau_n^{+}-\tau_n^{-}) \tag{2}$$

are the reflection and transmission coefficients with the atom in the upper or lower state, as indicated in Fig. 1.

In this section expressions for the dressed-state reflection and transmission coefficients (ρ and τ) are given for two

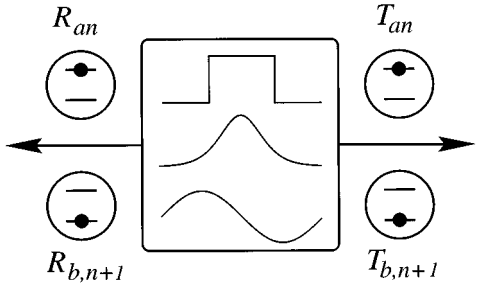

FIG. 1. Schematic drawing of the setup. The initial state is $|a,n\rangle$, i.e., the atoms are in the excited state and the field is in a number state. We consider three different mode functions, a mesa function, a sech^2, and a sinusoidal mode function. After the interaction the atoms are either transmitted or reflected and can be in the upper or lower state. This is described by the transmission and reflection coefficients R and T as indicated in the figure.

different mode functions: the mesa mode function and the sech^2 mode function. As the latter is smooth, it leads to a somewhat different behavior of the mazer. From these expressions and with Eq. (2), the bare-state reflection and transmission coefficients (R and T) are obtained.

The steady-state photon distribution for a mazer pumped by a Poissonian beam of atoms with the rate r is given by (see paper I)

$$P(n)=P(0)\prod_{m=1}^{n}\frac{Cn_{\mathrm{b}}+rP_{\mathrm{emission}}(m-1)/m}{C(n_{\mathrm{b}}+1)}, \tag{3}$$

where C is the cavity decay rate and n_{b} is the number of photons in thermal equilibrium.

A. Mesa function

In the special case, where the atom-field coupling inside the cavity is constant along the propagation axis of the atoms, e.g., for a TM mode in a cylindrical cavity, the reflection and transmission coefficients can be calculated analytically, as discussed in paper I. The mode function is then given by the mesa function

$$u(z)=\begin{cases}1 & \text{for } 0<z<L\\ 0 & \text{elsewhere,}\end{cases} \tag{4}$$

where L is the length of the cavity in the z direction. We obtain

$$\rho_n^{\pm}=i\Delta_n^{\pm}\sin(k_n^{\pm}L)\,\tau_n^{\pm},$$

$$\tau_n^{\pm}=[\cos(k_n^{\pm}L)-i\Sigma_n^{\pm}\sin(k_n^{\pm}L)]^{-1}, \tag{5}$$

where

$$k_n^{\pm}=(k^2\mp\kappa_n^2)^{1/2},$$

$$\Delta_n^{\pm}=\frac{1}{2}\left(\frac{k_n^{\pm}}{k}-\frac{k}{k_n^{\pm}}\right),$$

$$\Sigma_n^{\pm}=\frac{1}{2}\left(\frac{k_n^{\pm}}{k}+\frac{k}{k_n^{\pm}}\right), \tag{6}$$

$$\kappa=\sqrt{2Mg/\hbar},$$

$$\kappa_n=\kappa\sqrt[4]{n+1},$$

with the atomic mass M and the atom-field coupling strength g. The emission probability shows resonances as a function of κ_nL. This behavior is illustrated in Fig. 2(a). The resonances occur at $\kappa_nL=m\pi$ ($m=1,2,3,\ldots$), if the cavity contains n photons.

B. sech^2 function

In the following, we consider a sech^2 mode function

$$u(z)=\mathrm{sech}^2(z/L). \tag{7}$$

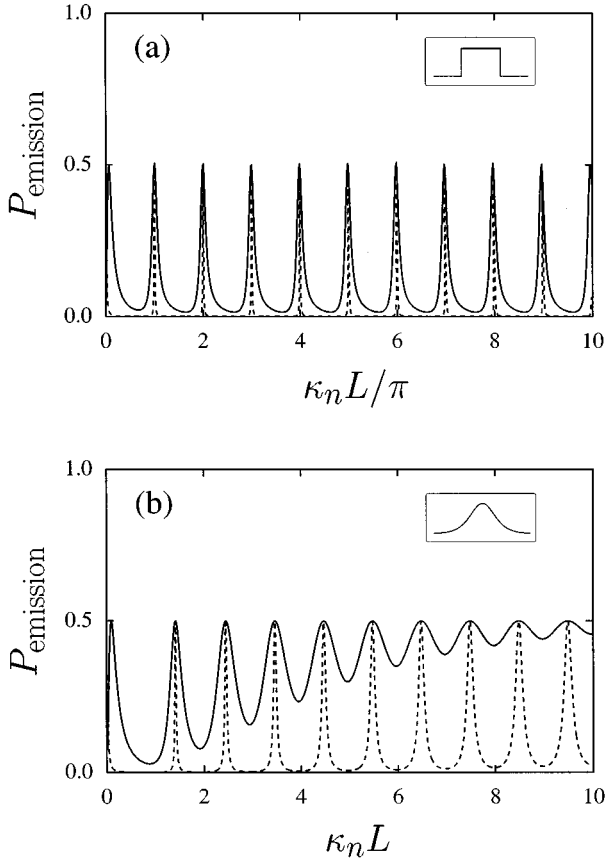

FIG. 2. The emission probability P_{emission} vs the interaction length κ_nL for $k/\kappa_n=0.01$ (solid) and $k/\kappa_n=0.1$ (dashed). (a) Mesa mode function and (b) sech^2 mode function.

This potential can be used as an approximation for a Gaussian mode in an optical resonator. The reflection and transmission coefficients are given by (see Appendix A for details)

$$\rho_n^{\pm}=\frac{\Gamma(ikL)\Gamma(1-ikL)}{\Gamma(1/2+i\xi_n^{\pm})\Gamma(1/2-i\xi_n^{\pm})}\,\tau_n^{\pm},$$

$$\tau_n^{\pm}=\frac{\Gamma[1/2-i(kL+\xi_n^{\pm})]\Gamma[1/2-i(kL-\xi_n^{\pm})]}{\Gamma(-ikL)\Gamma(1-ikL)}, \tag{8}$$

where

$$\xi_n^{\pm}=\sqrt{\pm(\kappa_nL)^2-1/4}. \tag{9}$$

As for the mesa function, P_{emission} shows resonances as a function of κ_nL for very slow atoms as illustrated in Fig. 2(b). There are, however, two major differences. First, the resonance condition is $\kappa_nL=\sqrt{m(m+1)}$ ($m=1,2,3,\ldots$), as compared to $\kappa_nL=m\pi$ for the mesa function. Second, for larger values of κ_nL the resonances become less pronounced and the emission probability approaches a plateau with $P_{\mathrm{emission}}=1/2$.

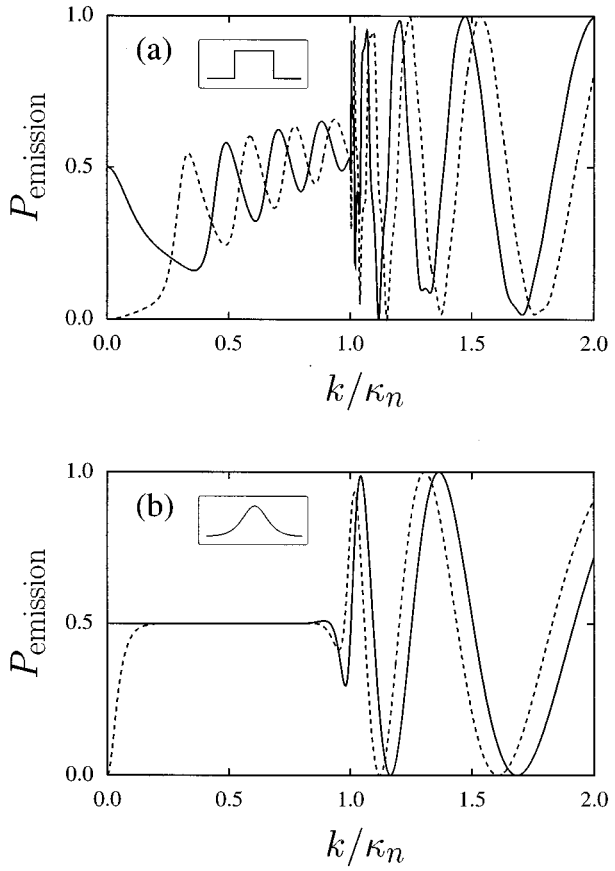

FIG. 3. The emission probability P_{emission} as a function of k/κ_n on a mazer resonance (solid curves) and between resonances (dashed curves). (a) Mesa function with $\kappa_n L = 10\pi$ (solid) and $\kappa_n L = 10.5\pi$ (dashed) and (b) sech^2 potential with $\kappa_n L = 10$ (solid) and $\kappa_n L = \sqrt{10(10+1)}$ (dashed).

C. Velocity regimes and emission probability

Depending on the velocity of the atoms, we distinguish three regimes: for $k \gg \kappa_n$ the CM motion is essentially classical and the kinetic term in the Hamiltonian can be neglected; therefore the standard micromaser theory applies. We call this regime the *Rabi regime*. If $k \ll \kappa_n$ the mazer resonances mentioned above occur. The quantized nature of the CM motion plays a crucial role. We call this regime the *mazer regime*. The parameter range where $k \simeq \kappa_n$ we call *intermediate regime*; this will be discussed in Sec. II C 2.

1. Mazer regime

In this section we want to discuss the features of the mazer regime and compare it to the well-known Rabi regime. Figure 3 shows a plot of P_{emission} as a function of k/κ_n both for the mesa (a) and for the sech^2 (b) potential. For $k > \kappa_n$ both potentials show a Rabi-like behavior. At $k \simeq \kappa_n$ a dramatic change happens. This change is abrupt for the mesa mode function and continuous for the sech^2 mode function. The physical reason for this is the following: for the mesa mode function tunneling does not play an essential role. The dressed-state component $|\gamma_{n+1}^{+}\rangle$, which encounters the potential well, is completely reflected as long as $k < \kappa$. If k becomes larger than κ, it is suddenly transmitted. The sech^2 potential, on the other hand, forms a narrower well for energies that are a little bit smaller than the maximal atom-field interaction energy. Therefore, there is a substantial tunneling probability if k is smaller but on the order of κ, which smears out the sudden change of P_{emission} at $k = \kappa$. For very slow atoms, i.e., for $k \ll \kappa_n$ the behavior is similar for both potentials: On a mazer resonance $P_{\text{emission}} = 1/2$ (solid curves), between the resonances $P_{\text{emission}} = 0$ (dashed curves). As already noted, the resonance condition is $\kappa_n L = m\pi$ for the mesa potential and $\kappa_n L = \sqrt{m(m+1)}$ for the sech^2 potential, if the cavity contains n photons.

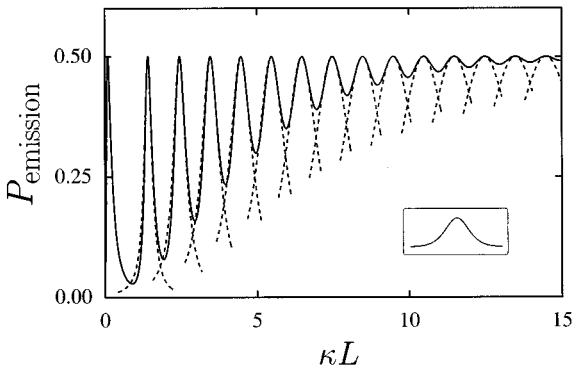

FIG. 4. Exact emission probability P_{emission} (solid) vs the interaction length κL for $k/\kappa = 0.1$. The expansion around each resonance (dashed) shows that the width of the resonances increases with larger κL.

To get a deeper insight into the behavior of the resonances in both cases, we consider the case $n = 0$, introduce a variable d that is a measure of the distance of κL from the resonance scaled by k/κ, use the expansion

$$\kappa L = m\pi + d\frac{k}{\kappa}, \tag{10}$$

and take the limit $k/\kappa \to 0$. Details are given in Appendix C. The result is the emission probability

$$P_{\text{emission}}(0) = \frac{1}{2}\frac{1}{1+d^2/4}, \tag{11}$$

which is a Lorentzian. All resonances have the same width, independent of the order m of the resonance.

For the sech^2 function, we obtain with a similar expansion

$$\kappa L = \sqrt{m(m+1)} + d\frac{k}{\kappa} \tag{12}$$

and the emission probability

$$P_{\text{emission}}(0) = \frac{1}{2}\frac{(2m+1)^2}{(2m+1)^2+4d^2}. \tag{13}$$

Note that in this case the emission probability is also a Lorentzian, but now the width growths with increasing order m. This is illustrated in Fig. 4 where we plot the exact emission probability using Eqs. (1), (2), and (5), as well as the expansions (13) at each resonance. For small values of κL the resonances are well separated. The expansion fits the

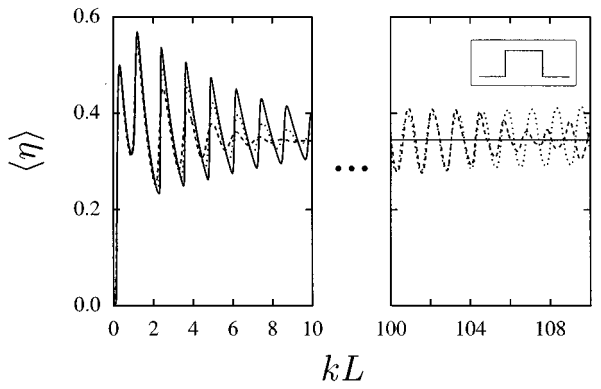

FIG. 5. Normalized steady-state photon number $\langle \eta \rangle$ as a function of kL in the intermediate regime ($\kappa/k\sqrt[4]{N_{\rm ex}}=3$) for $N_{\rm ex}=20$ (dotted), $N_{\rm ex}=50$ (dashed), and $N_{\rm ex}\to\infty$ (solid).

sharply peaked resonances. For larger values of κL, the resonances start to overlap, and the emission probability approaches its asymptotic value of 1/2.

2. Intermediate regime

The intermediate regime is characterized by the fact that neither $k/\kappa_n \gg 1$ as in the Rabi limit nor $k/\kappa_n \ll 1$ as in the mazer limit.

For the mesa mode function [Fig. 3(a)], there are oscillations around a mean value that is decreasing with decreasing k/κ_n. For the sech^2 mode function [Fig. 3(b)], on the other hand, there is a plateau with $P_{\rm emission}(n)=1/2$ for a wide range of k values. Note that within the plateau all of the probabilities under consideration are the same: $|T_{an}|^2=|T_{b,n+1}|^2=|R_{an}|^2=|R_{b,n+1}|^2=1/4$. This means half of the atoms are reflected, half are transmitted, and the emission probability for each atom is 1/2, regardless of whether it is transmitted or reflected. In this case and for small $n_{\rm b}$, the field generated in the cavity has a Poissonian distribution

$$P(n)=\frac{P(0)}{n!}\left(\frac{r}{2C}\right)^n \tag{14}$$

with a mean photon number $\langle a^\dagger a\rangle = r/2C$. Such a distribution is not found in the usual micromaser.

In the intermediate regime neither $\theta=\sqrt{N_{\rm ex}}g\tau_{\rm int}$ ($N_{\rm ex}=r/C$ being the scaled pumping rate and $\tau_{\rm int}$ the interaction time) nor $\kappa_n L$ describe the steady state in the clearest way. We introduce the normalized photon number $\eta \equiv n/N_{\rm ex}$, the scaling parameter $\mu \equiv \sqrt[4]{N_{\rm ex}}\kappa/k$, and the interaction length kL as the natural parameters of the intermediate regime. Figure 5 shows a plot of the normalized mean photon number $\langle \eta \rangle = \langle n \rangle / N_{\rm ex}$ versus kL for different values of the pumping rate $N_{\rm ex}$ for the mesa mode function, keeping the scaling parameter μ fixed. Note that in the limit $N_{\rm ex}\to\infty$, the steady-state photon number tends towards an asymptotic curve (solid line) with sharp peaks at approximately equal distances for small values of kL (left panel of Fig. 5), and for large kL a constant value is reached (right panel of Fig. 5). The behavior for large kL is due to the fact that several Fock states contribute to $\langle n \rangle$ and therefore the different emission probabilities $P_{\rm emission}(n)$ lead to an irregular dependence on kL.

With the introduction of the scaling parameters θ and η, we can analyze the equations governing the mazer. In the case $\eta \gg 1/N_{\rm ex}$, $k/\kappa_n \simeq 1$, we get with Eq. (5)

$$\begin{aligned} \tau_\eta^+ &\simeq 0, \\ \rho_\eta^+ &\simeq 1, \\ \tau_\eta^- &\simeq \left[\cos(\mu\sqrt[4]{\eta}kL)-\frac{i}{2}\mu\sqrt[4]{\eta}\sin(\mu\sqrt[4]{\eta}kL)\right]^{-1}, \\ \rho_\eta^- &\simeq \frac{i}{2}\mu\sqrt[4]{\eta}\sin(\mu\sqrt[4]{\eta}kL)\,\tau_\eta^-. \end{aligned} \tag{15}$$

This means that the $|\gamma_{n+1}^+\rangle$ component is completely reflected. The $|\gamma_{n+1}^-\rangle$ component is partially transmitted and partially reflected. The reflection and transmission amplitudes for the $|\gamma_{n+1}^-\rangle$ component are periodic as a function of kL with the period $2\pi/(\mu\sqrt[4]{\eta})$; see Fig. 5. The fading of the oscillations with larger kL can be explained by the fact that a larger value of kL causes faster oscillations in the scaled photon number η. Since several values of η contribute to $\langle n \rangle$, this causes an averaging that results in a collapse of the oscillations in $\langle n \rangle$.

III. SINUSOIDAL MODE FUNCTIONS

When the cavity mode is described by a sinusoidal mode function as in a TE mode instead of the mesa function (4), which describes a TM mode, the reflection and transmission coefficients change and the emission probability is modified. We here present a detailed Wentzel-Kramers-Brillouin calculation for such a case. In each of the regions that are distinguished in Fig. 6, taking the sharp corners of the potential at the ports of the cavity into account, we make an ansatz for the wave function of the form

$$\begin{aligned} \psi(z) = {} & A_j K(z)^{-1/2}\exp\left(i\int_{a_j}^{z}K(z)dz\right) \\ & + B_j K(z)^{-1/2}\exp\left(-i\int_{a_j}^{z}K(z)dz\right), \end{aligned} \tag{16}$$

where $K(z)=\sqrt{2M[E-V(z)]}/\hbar$. At the sharp corners, we demand the continuity of the wave function and its first derivative. At the turning points, the well-known connection formulas are used [5]. The WKB approximation is applicable if

$$\left|\frac{1}{2}\chi\frac{d^2\chi}{dz^2}-\frac{1}{4}\left(\frac{d\chi}{dz}\right)^2\right| \ll 1 \tag{17}$$

with $\chi(z)=K(z)^{-1}$. This condition is fulfilled, for example, when $\kappa L \gg 1$ as for usual micromaser cavities.

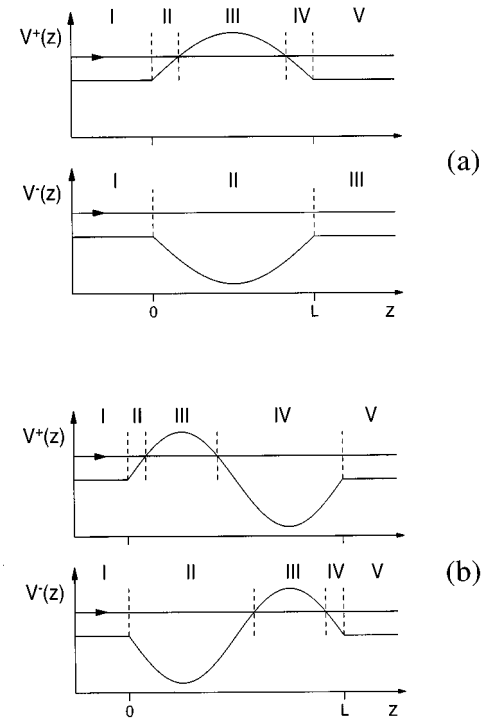

FIG. 6. Schematic representation of sinusoidal mode functions and the regions that are distinguished in the WKB calculation for (a) the fundamental mode and (b) the second harmonic mode.

A. Fundamental mode

The fundamental sinusoidal mode is described by the mode function

$$u(z)=\begin{cases}\sin(\pi z/L) & \text{for } 0<z<L\\ 0 & \text{elsewhere,}\end{cases} \tag{18}$$

which is shown in Fig. 6(a). Two cases have to be distinguished.

1. Case: $k>\kappa_n$

The reflection and transmission coefficients are for $k>\kappa_n$

$$\rho_n^{\pm}=\pm 2i\eta_n[\cos(\varphi_n^{\pm})\mp\eta_n\sin(\varphi_n^{\pm})]\tau_n^{\pm},$$
$$\tau_n^{\pm}=[\eta_n^2 e^{i\varphi_n^{\pm}}+(1\mp i\eta_n)^2 e^{-i\varphi_n^{\pm}}]^{-1}, \tag{19}$$

with the phase integrals

$$\varphi_n^{\pm}=\frac{2L}{\pi}\int_0^{\pi/2}\sqrt{k^2\mp\kappa_n^2\cos(z)}\,dz \tag{20}$$

and

$$\eta_n=\left|\frac{dK}{dz}(0)\right|\left(\frac{1}{2k}\right)^2=\frac{\pi\kappa_n^2}{8k^3L}. \tag{21}$$

An analytical expression for this phase integral is given in Appendix B in terms of the elliptic integrals of the first and second kind [6]

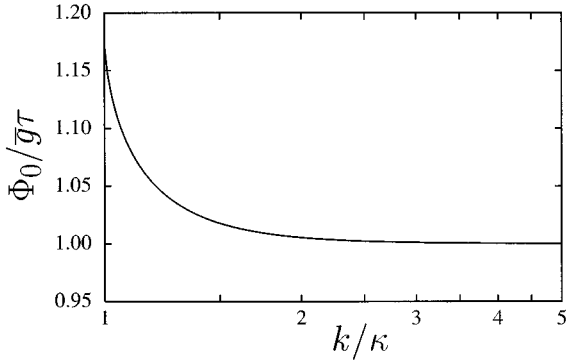

FIG. 7. The phase Φ_0 in the long-cavity limit as a function of the atomic momentum k for the fundamental sinusoidal mode.

$$F(x,y)=\int_0^x\frac{d\theta}{\sqrt{1-y^2\sin^2(\theta)}},$$
$$E(x,y)=\int_0^x\sqrt{1-y^2\sin^2(\theta)}\,d\theta. \tag{22}$$

In the limit of very fast atoms, we regain the Rabi oscillations. Their period is determined by the average atom-field coupling $\bar{g}=2g/\pi$ in agreement with the result of Ref. [7].

The limit of large L corresponds to $\eta_n\to 0$. In this case the expression for the emission probability simplifies to

$$P_{\text{emission}}(n)=\sin^2(\Phi_n) \tag{23}$$

with the phase

$$\Phi_n=\frac{2L}{\pi}\left(\sqrt{k^2+\kappa_n^2}[E(\delta,b)-E(\pi/4,b)]-\frac{\kappa_n}{k}\right), \tag{24}$$

where $b=[2\kappa_n^2/(\kappa_n^2+k^2)]^{1/2}$ and $\delta=\arcsin(\kappa_n/bk)$. The dependence of this phase on k/κ is illustrated in Fig. 7.

2. Case: $k<\kappa_n$

For very slow atoms ($k<\kappa_n$), we obtain

$$\rho_n^{+}=i\left\{2\eta_n[\cos(2\chi_n^{+})-\eta_n\sin(2\chi_n^{+})]\left(e^{\tilde{\chi}_n^{+}}+\frac{e^{-\tilde{\chi}_n^{+}}}{4}\right)-(1+2\eta_n^2)\left(e^{\tilde{\chi}_n^{+}}-\frac{e^{-\tilde{\chi}_n^{+}}}{4}\right)\right\}\tau_n^{+},$$
$$\tau_n^{+}=\left\{e^{\tilde{\chi}_n^{+}}[(1-i\eta_n)e^{-i\chi_n^{+}}-\eta_n e^{i\chi_n^{+}}]^2+\frac{e^{-\tilde{\chi}_n^{+}}}{4}[(1-i\eta_n)e^{-i\chi_n^{+}}+\eta_n e^{i\chi_n^{+}}]^2\right\}^{-1} \tag{25}$$
$$\rho_n^{-}=-2i\eta_n[\cos(\chi_n^{-})+\eta_n\sin(\chi_n^{-})]\tau_n^{-},$$
$$\tau_n^{-}=[\eta_n^2 e^{i\chi_n^{-}}+(1+i\eta_n)^2 e^{-i\chi_n^{-}}]^{-1}$$

with

$$\chi_n^+ = \frac{L}{\pi}\int_a^{\pi/2} \sqrt{k^2 - \kappa_n^2 \cos(z)}\, dz,$$

$$\tilde{\chi}_n^+ = \frac{2L}{\pi}\int_0^{a} \sqrt{\kappa_n^2 \cos(z) - k^2}\, dz, \tag{26}$$

$$\chi_n^- = \varphi_n^-,$$

where $a = \arccos(k^2/\kappa_n^2)$ and η_n as in Eq. (21). Analytical expressions for these phase integrals are given in Appendix B.

For large values of L, we have $\eta_n \to 0$ and $\tilde{\chi}_n^+ \to \infty$. In this case, the emission probability is always 1/2, independent of the number of photons in the cavity (if the relevant values of n are not too large), and for small n_b the field generated in the cavity has a Poissonian distribution, as discussed above for the sech^2 potential [Eq. (14)].

B. Second harmonic mode

Finally, we consider the sinusoidal mode function

$$u(z) = \begin{cases} \sin(2\pi z/L) & \text{for } 0 < z < L \\ 0 & \text{elsewhere,} \end{cases} \tag{27}$$

which is depicted in Fig. 6(b).

For large values of L and $k < \kappa_n$, we obtain, using the ansatz (16),

$$\rho_n^{\pm} = -i \exp(2i\phi_n^{\pm}),$$

$$\tau_n^{\pm} = 0 \tag{28}$$

with the phase integrals

$$\phi_n^+ = \frac{L}{2\pi}\int_{x_0}^{\pi/2} \sqrt{k^2 - \kappa_n^2 \cos(z)}\, dz,$$

$$\phi_n^- = \phi_n^+ + \Delta_n, \tag{29}$$

and the phase difference

$$\Delta_n = \frac{L}{\pi}\int_0^{\pi/2} \sqrt{k^2 + \kappa_n^2 \cos(z)}\, dz. \tag{30}$$

Analytical solutions for these integrals are given in Appendix B. We have introduced the short-hand notations $x_0 = \arccos(k^2/\kappa_n^2)$, $f = [2\kappa_n^2/(\kappa_n^2 + k^2)]^{1/2}$, $\alpha = \arcsin(1/f)$, and $\beta = \arcsin(f/\sqrt{2})$.

Equation (28) implies that the incident atom is always reflected. Half of the time, it encounters immediately a potential barrier and is reflected. However, when it first encounters the attractive part of the sinusoidal potential, the atomic wave function can pick up an additional phase before the atom is reflected off the repulsive part of the potential. This additional phase varies with the length of the cavity and gives rise to the emission probability

$$P_{\text{emission}}(n) = \sin^2(\Delta_n) \tag{31}$$

with the phase

$$\Delta_n = \phi_n^- - \phi_n^+ . \tag{32}$$

The incident excited atoms deposit a photon into the cavity with a fixed probability, which can take on any value between zero and one, depending on the length of the cavity. In particular, the cavity length can be such that all the atoms deposit a photon into the cavity while they are reflected. The cavity field acts as a mirror that may or may not change the internal state of the incident atoms in addition to reflecting them. We can build state-changing and state-preserving mirrors for atoms.

IV. EXPERIMENTAL CONSIDERATIONS

A. Micromaser

In this section we want to discuss how a mazer-type experiment could be performed with the one-atom maser setup [3]. We consider the transition $63P_{3/2} \to 61P_{5/2}$ in ^{85}Rb used in the Garching experiments. The typical parameters are $g = 44$ kHz, $M = 1.4 \times 10^{-25}$ kg, and $L = 2.5$ cm. This yields $\kappa_n = 1.1 \times 10^7$ m^{-1}. To reach the mazer regime with the cavity field being the vacuum, we therefore need a velocity $v < 8$ mm/s, corresponding to a temperature of about 100 nK, which is in the range of state-of-the-art cooling techniques [8]. By injecting a microwave field into the cavity and therefore enhancing the potential, one could, however, use faster atoms.

As the de Broglie wavelength of the atoms for the parameters under consideration is in the μm range, it should be possible to realize a mesalike potential with a TM mode. To see the sharp resonances in P_{emission} requires, however, an extremely narrow velocity distribution of the atoms. This is due to the large value of $\kappa_n L \simeq 10^5$. The argument of the sine and cosine functions in the expressions for $\rho_n^{\pm}$ and $\tau_n^{\pm}$ in Eq. (5) is $k_n^{\pm} L$. If the velocity is given by $v = v_0 + \delta v$, where $v_0 = k_0/M$ is the mean velocity and δv is a small velocity spread, there is also a small spread $\delta k_n^{\pm}$. To see the resonances, $\delta k_n^{\pm} L < \pi/2$ is required, which implies $\delta v/v = 6 \times 10^{-4}$ for $k/\kappa_n = 0.1$. This is several orders of magnitude smaller than the state of the art in the experiments.

Therefore an averaging over a small velocity range [9] has to be performed to describe the experimental situation. This leads to

$$\overline{P}_{\text{emission}} = \frac{1}{2}\left[1 - \frac{(\kappa_n^2 + k_0^2)^{1/2} - k_0}{(\kappa_n^2 + k_0^2)^{1/2} + k_0} \frac{\kappa_n^2}{2k_0(\kappa_n^2 - k_0^2)^{1/2} - 2k_0^2 + \kappa_n^2}\right]. \tag{33}$$

Owing to this averaging, the sharp resonances in P_{emission} as a function of $\kappa_n L$ are smeared out and the emission probability is constant in the mazer regime. This is, however, still very different from the oscillations in the Rabi regime as it leads to a Poissonian photon distribution [Eq. (14)] as discussed for the sech^2 and sinusoidal mode functions.

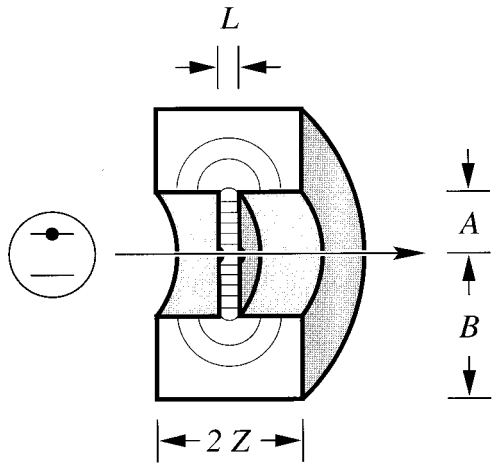

FIG. 8. Schematic drawing of a possible setup. Atoms in the excited state travel along the z axis. The cavity is of the reentrant type and has a cylindrical symmetry around the z axis. The lines inside the cavity represent the electric field lines.

B. Microlaser

The recent developments of high-Q optical cavities make a mazer-type experiment in the optical domain feasible. The advantage of such an experiment compared to the microwave regime is that due to the small mode volume a larger coupling constant g can be achieved, which allows for larger κ_n and therefore for larger velocities. To give an estimate for the velocities needed, we consider a cavity of length $L=1$ mm and the TEM_{00} mode with a beam waist of $w_0=10$ μm, resulting in a mode volume of $V=1.6\times10^{-13}$ m^{-3}. Using rubidium atoms and the D_2 line as the transition under consideration, this yields a coupling constant $g=200$ MHz and $\kappa_n=7\times10^8$ m^{-1}. To fulfill $k<\kappa_n$, we need a velocity $v<0.5$ m/s, which corresponds to a temperature in the mK range.

C. Reentrant cavity

In order to see most clearly the mazer resonances, also when the atoms have a certain velocity spread, the parameter κL has to be small, as discussed in Sec. IV A. This can be achieved in the setup shown in Fig. 8. This cavity is of the reentrant type [10–12], which allows for a very small interaction length L. As the field inside the interaction region is homogeneous [13], it is given by a mesa mode function, independent of the wavelength λ.

The resonant wavelength and the Q value can be approximated by [11]

$$\lambda_{\mathrm{res}}\simeq 2\pi\sqrt{\frac{ZA^2}{L}\ln(B/A)}, \tag{34}$$

$$Q=\frac{\mu_0\omega}{R}G, \tag{35}$$

with the vacuum permeability μ_0, the transition (circular) frequency ω, the high-frequency resistance R, and a geometry factor G, which is defined as the ratio of a volume integral and a surface integral

$$G=\frac{\int dVH^2}{\oint dSH^2}, \tag{36}$$

where H is the magnetic field. For the cavity proposed here, one finds [11]

$$G\simeq\frac{(Z/\lambda)\ln(B/A)}{(Z/A)(1+A/B)+\ln(B/A)}. \tag{37}$$

To estimate whether this setup can be realized experimentally, we consider the transition $63P_{3/2}\rightarrow 61P_{5/2}$ in ^{85}Rb with $\omega=2\pi\times21$ GHz as in Sec. IV A. With the parameters $L=100$ μm, $A=2.0$ mm, $B=3.0$ mm, and $Z=4.0$ mm, Eq. (34) yields the resonant wavelength $\lambda_{\mathrm{res}}=5$ cm, which corresponds to the transition under consideration. For this geometry we have $G=4.34\times10^{-4}$ m. For a superconducting Nb resonator with $R=80$ $\mu\Omega$, this yields Q on the order of 10^6.

If we assume the same coupling constant $g=44$ kHz as in the Garching micromaser (Sec. IV A), we have $\kappa\simeq10^7$ m^{-1} and therefore $\kappa L\simeq10^3$. For $k/\kappa=0.1$ we therefore need a velocity selection of about $\delta v/v=15\%$ in order to see the mazer resonances. In the present Garching setup, the velocity selectivity is about 1.5%. This should allow one to see the resonances very clearly. On the other hand, with this velocity spread one could use more convenient cavity dimensions, e.g., $L=1.0$ mm, $A=4.0$ mm, $B=6.5$ mm, and $Z=8.0$ mm.

In conclusion we see that an experiment with realistic parameters seems possible.

V. SUMMARY AND DISCUSSION

We have considered a micromaser pumped by slow atoms. If the kinetic energy of the atoms is comparable to the atom-field interaction energy, effects of the quantized CM motion are important. The emission probability and the photon statistics change dramatically, even for realistic experimental parameters.

We have reviewed the quantum theory of the mazer and given exact analytical results for a mesa and a sech^2 mode function, as well as WKB solutions for sinusoidal modes. For a mesa mode function, sharp resonances in the emission probability as a function of the interaction length occur, leading to unusual photon distributions. For small values of κL also the sech^2 potential yields the mazer resonances, for larger values both the sech^2 and sinusoidal mode functions show a plateau with constant emission probability leading to Poissonian photon distributions. For the sinusoidal mode functions interesting features are found such as the possibility to build a state-changing or state-preserving atomic mirror. In all cases, the mazer regime is very different from the well-known Rabi regime.

Various possibilities for experimental realizations have been presented, showing that it should be possible to see mazer action experimentally. The most promising setup is a microwave cavity of the reentrant type, as for such a cavity the interaction length can be on the order of the de Broglie wavelength of the pumping atoms.

ACKNOWLEDGMENTS

This work has been supported by the Office of Naval Research, the Welch Foundation, and the Texas Advanced Research Program. One of us (M. Sch.) gratefully thanks the Studienstiftung des deutschen Volkes for support.

APPENDIX A: CALCULATION FOR sech^2 POTENTIAL

The reflection and transmission coefficients for the potential

$$V_n^{\pm}(z)=\pm\hbar g\sqrt{n+1}u(z) \tag{A1}$$

with

$$u(z)=\mathrm{sech}^2(z/L) \tag{A2}$$

can be calculated analytically [14]. For convenience, we rewrite the potential as

$$V_n^{\pm}(z)=\frac{\hbar^2}{2ML^2}\frac{\xi_n^{\pm 2}+1/4}{\cosh^2(z/L)} \tag{A3}$$

with

$$\xi_n^{\pm}=\sqrt{\pm(\kappa_n L)^2-1/4} \tag{A4}$$

and obtain the time-independent Schrödinger equation

$$\left[\frac{d^2}{dz^2}+k^2-\frac{\xi_n^{\pm 2}+1/4}{L^2\cosh^2(z/L)}\right]\psi_n^{\pm}(z)=0 \tag{A5}$$

for the corresponding scattering problem. The transformation $x=[1+\exp(2z/L)]^{-1}$ leads to

$$\left[x(1-x)\frac{d^2}{dx^2}+(1-2x)\frac{d}{dx}+\frac{k^2L^2}{4x(1-x)}-(\xi_n^{\pm 2}+1/4)\right]\psi_n^{\pm}(x)=0. \tag{A6}$$

The ansatz $\psi_n^{\pm}(x)=x^p(1-x)^q f(x)$ yields the hypergeometric differential equation

$$x(1-x)\frac{d^2}{dx^2}f(x)+[2p+1-2(p+q+1)x]\frac{d}{dx}f(x)-[(p+q+1/2)^2+\xi_n^{\pm 2}]f(x)=0, \tag{A7}$$

which is solved by the hypergeometric function

$$f(x)={}_2F_1(\alpha,\beta,\gamma;x)=\sum_{n=0}^{\infty}\frac{z^n}{n!}\prod_{k=0}^{n-1}\frac{(\alpha+k)(\beta+k)}{\gamma+k}, \tag{A8}$$

where $p^2+(kL/2)^2=0$, $p^2=q^2$, and

$$\alpha=(p+q+1/2)+i\xi_n^{\pm},\qquad \beta=(p+q+1/2)-i\xi_n^{\pm},\qquad \gamma=2p+1. \tag{A9}$$

To select one of the four possible sign combinations for p and q and to find the reflection and transmission coefficients, we consider the boundary conditions

$$\psi_n^{\pm}(z)=\begin{cases}\exp(ikz)+\rho_n^{\pm}\exp(-ikz) & \text{for } z\to-\infty\\ \tau_n^{\pm}\exp(ikz) & \text{for } z\to\infty.\end{cases} \tag{A10}$$

For convenience, we have used here a different phase convention for $\tau_n^{\pm}$ compared to Eq. (9) in paper I.

In the limit $z\to\infty$, we obtain $x\simeq\exp(-2z/L)\ll 1$ and therefore $\psi_n^{\pm}(x)\simeq Cx^p=C\exp(-2pz/L)$, which implies $\tau_n^{\pm}=C$ and $p=-ikL/2$. For the limit $z\to-\infty$, on the other hand, we obtain $1-x\simeq\exp(2z/L)\ll 1$, and using $\gamma-\alpha-\beta=-2q$ and

$$\begin{aligned}{}_2F_1(\alpha,\beta,\gamma;x)=&\frac{\Gamma(\gamma)\Gamma(\gamma-\alpha-\beta)}{\Gamma(\gamma-\alpha)\Gamma(\gamma-\beta)}\\ &\times{}_2F_1(\alpha,\beta,\alpha+\beta-\gamma+1;1-x)\\ &+(1-x)^{\gamma-\alpha-\beta}\frac{\Gamma(\gamma)\Gamma(\alpha+\beta-\gamma)}{\Gamma(\alpha)\Gamma(\beta)}\\ &\times{}_2F_1(\gamma-\alpha,\gamma-\beta,\gamma-\alpha-\beta+1;1-x),\end{aligned} \tag{A11}$$

we find

$$\psi_n^{\pm}(z)=C\left[\frac{\Gamma(\gamma)\Gamma(\gamma-\alpha-\beta)}{\Gamma(\gamma-\alpha)\Gamma(\gamma-\beta)}\exp(2qz/L)+\frac{\Gamma(\gamma)\Gamma(\alpha+\beta-\gamma)}{\Gamma(\alpha)\Gamma(\beta)}\exp(-2qz/L)\right]. \tag{A12}$$

Therefore the sign of q is arbitrary, it only changes the role of the coefficients in Eq. (A12); we choose $q=-p=ikL/2$. Finally, by comparing Eqs. (A10) and (A11), we obtain the reflection and transmission coefficients

$$\rho_n^{\pm}=\frac{\Gamma(ikL)\Gamma[1/2-i(kL+\xi_n^{\pm})]\Gamma[1/2-i(kL-\xi_n^{\pm})]}{\Gamma(-ikL)\Gamma(1/2+i\xi_n^{\pm})\Gamma(1/2-i\xi_n^{\pm})},$$

$$\tau_n^{\pm}=\frac{\Gamma[1/2-i(kL+\xi_n^{\pm})]\Gamma[1/2-i(kL-\xi_n^{\pm})]}{\Gamma(-ikL)\Gamma(1-ikL)}. \tag{A13}$$

APPENDIX B: PHASE INTEGRALS

For the phase integrals (20), (26), and (29), analytical expressions can be found [15] in terms of the elliptic integrals of the first and second kind.

1. Fundamental mode

For $k>\kappa_n$, we obtain

$$\varphi_n^+=\frac{2L}{\pi}\int_0^{\pi/2}\sqrt{k^2-\kappa_n^2\cos(z)}dz$$
$$=\frac{2L}{\pi}\left[2\sqrt{k^2+\kappa_n^2}E(\delta,b)-\frac{2\kappa_n^2}{k}\right],$$
$$\varphi_n^-=\frac{2L}{\pi}\int_0^{\pi/2}\sqrt{k^2-\kappa_n^2\cos(z)}dz$$
$$=\frac{4L}{\pi}\sqrt{k^2+\kappa_n^2}E(\pi/4,b). \tag{B1}$$

For $k<\kappa_n$, we obtain

$$\chi_n^+=\frac{L}{\pi}\int_a^{\pi/2}\sqrt{k^2-\kappa_n^2\cos(z)}dz$$
$$=\frac{\kappa_nL}{\pi}\sqrt{2}\{2[E(\pi/4,b)-E(\alpha,b)]$$
$$+(1-k^2/\kappa_n^2)[F(\alpha,b)-F(\pi/4,b)]\},$$
$$\tilde{\chi}_n^+=\frac{2L}{\pi}\int_0^{a}\sqrt{\kappa_n^2\cos(z)-k^2}dz$$
$$=\frac{2\kappa_nL}{\pi}\sqrt{2}[2E(\pi/2,1/b')-(k^2/\kappa_n^2+1)F(\pi/2,1/b')], \tag{B2}$$
$$\chi_n^-=\varphi_n^-.$$

Here we have introduced the short-hand notations $\alpha=\arcsin(1/b)$, $\gamma=\arcsin(b/\sqrt{2})$, and $b'=[2\kappa_n^2/(\kappa_n^2-k^2)]^{1/2}$.

2. Second harmonic mode

For the second harmonic mode and for $k<\kappa_n$, we obtain the phase integrals

$$\phi_n^+=\frac{L}{2\pi}\int_{a'}^{\pi/2}\sqrt{k^2-\kappa_n^2\cos(z)}dz$$
$$=\kappa_nL\frac{\sqrt{2}}{2\pi}\{2[E(\pi/4,f)-E(\alpha,f)]$$
$$-(1-k^2/\kappa_n^2)[F(\pi/4,f)-F(\alpha,f)]\},$$
$$\phi_n^-=\phi_n^++\Delta_n \tag{B3}$$

with the phase difference

$$\Delta_n=\frac{L}{\pi}\int_0^{\pi/2}\sqrt{k^2+\kappa_n^2\cos(z)}dz$$
$$=\kappa_nL\frac{\sqrt{2}}{\pi}[2E(\beta,1/f)-(1-k^2/\kappa_n^2)F(\beta,1/f)]. \tag{B4}$$

Here we have introduced the short-hand notations $a'=\arccos(k^2/\kappa_n^2)$, $f=[2\kappa_n^2/(\kappa_n^2+k^2)]^{1/2}$, $\alpha=\arcsin(1/f)$, and $\beta=\arcsin(f/\sqrt{2})$.

APPENDIX C: EXPANSION NEAR THE MAZER RESONANCES

In this Appendix, we derive approximate expressions for the reflection and transmission coefficients $\rho_n^{\pm}$ and $\tau_n^{\pm}$ in the mazer limit and in the neighborhood of a resonance.

1. Mesa function

As discussed in detail in paper I, in the mazer limit the probability

$$P_{\text{emission}}(n)=\frac{\frac{1}{2}[1+\frac{1}{2}\sin(2\kappa_nL)]}{1+(\kappa_n/2k)^2\sin^2(\kappa_nL)} \tag{C1}$$

of emission of a photon in the presence of n cavity photons displays characteristic resonances at

$$\kappa_nL=m\pi. \tag{C2}$$

In general, the atom encounters a linear combination of several Fock states $|n\rangle$, and the resonance condition reads

$$\kappa L=\frac{m\pi}{\sqrt[4]{N}} \tag{C3}$$

with N and m being integer numbers. We label each resonance by (N,m).

In order to understand the behavior of $\rho_n^{\pm}$ and $\tau_n^{\pm}$ in the mazer limit around a particular (N,m) resonance, we make the ansatz

$$\kappa L=\frac{m\pi}{\sqrt[4]{N}}+d\frac{k}{\kappa}, \tag{C4}$$

that is, we introduce a quantity d, which specifies the distance of κL from the exact resonance scaled by k/κ. We substitute this ansatz into the expressions for $\rho_n^{\pm}$ and $\tau_n^{\pm}$ and take the limit $k/\kappa\to 0$. In this way, we get expressions that depend on the new variable d.

Here we note that in the limit $k/\kappa\to 0$ the quantity k_n^+ takes on imaginary values. Indeed we find from Eq. (6)

$$k_n^+\simeq i\kappa_n. \tag{C5}$$

We insert this expression into Eq. (5) and find for $k/\kappa\to 0$,

$$\tau_n^+\simeq\left[\cosh(\kappa_nL)+i\frac{\kappa_n}{2k}\sinh(\kappa_nL)\right]^{-1}\to 0,$$
$$\rho_n^+\simeq -i\frac{\kappa_n}{2k}\sinh(\kappa_nL)\tau_n^+\to -1 \tag{C6}$$

for the $|\gamma_n^+\rangle$ component.

For the scattering amplitudes of the $|\gamma_n^-\rangle$ component, k_n^- is real and we find

$$k_n^- \simeq \kappa_n . \tag{C7}$$

Now, we consider the case where we have the limit

$$\sin(k_n^- L) \to 0 \tag{C8}$$

for $k/\kappa \to 0$, i.e., $k_n^- L \to M\pi$ for an integer M. Then we obtain for $k/\kappa \to 0$, via inserting

$$\cos(k_n^- L) \simeq \cos\left(\frac{\sqrt[4]{n+1}}{\sqrt[4]{N}} m\pi + d\frac{k}{\kappa}\sqrt[4]{n+1} \right) \to (-1)^M \tag{C9}$$

and

$$\sin(k_n^- L) \simeq \sin\left(\frac{\sqrt[4]{n+1}}{\sqrt[4]{N}} m\pi + d\frac{k}{\kappa}\sqrt[4]{n+1} \right) \to (-1)^M d\frac{k}{\kappa}\sqrt[4]{n+1} \tag{C10}$$

into Eq. (5), the amplitudes of reflection and transmission of the $|\gamma_n^-\rangle$ component as

$$\rho_n^- = \frac{i\sqrt{n+1}d/2}{1 - i\sqrt{n+1}d/2},$$

$$\tau_n^- = \frac{(-1)^M}{1 - i\sqrt{n+1}d/2}. \tag{C11}$$

If instead of Eq. (C8) we have the limit

$$\sin(k_n^- L) \to \text{const} \neq 0 \tag{C12}$$

for $k/\kappa \to 0$, we get

$$\rho_n^- = -1 = \rho_n^+ ,$$

$$\tau_n^- = 0 = \tau_n^+ . \tag{C13}$$

At a given (N,m) resonance, that is, for a certain $\kappa L = m\pi/\sqrt[4]{N}$, the state of the atom-cavity system in general consists of several dressed-state components $\gamma_n^\pm$ corresponding to different potentials of heights $\pm\hbar g\sqrt{n+1}$. For each $|\gamma_n^-\rangle$, i.e., for each n, we have to check whether Eq. (C8) or Eq. (C12) holds. Since $k_n^- L \to m\pi\sqrt[4]{n+1}/\sqrt[4]{N}$, the condition (C8) is equivalent to

$$n = N\frac{M^4}{m^4} - 1. \tag{C14}$$

We denote the photon numbers n for which Eq. (C11) holds by n_{res}. For $n = n_{\text{res}}$ and $d = 0$, the $|\gamma_n^-\rangle$ component is resonantly transmitted whereas the $|\gamma_n^+\rangle$ component is reflected with amplitude -1. For all other photon numbers $n \neq n_{\text{res}}$, Eq. (C13) holds and both components are reflected with amplitude -1.

The emission probability is given by

$$P_{\text{emission}}(n) = \begin{cases} \frac{1}{2}\dfrac{1}{1+(n+1)d^2/4} & \text{for } n = n_{\text{res}} \\ 0 & \text{otherwise.} \end{cases} \tag{C15}$$

2. sech^2 function

In the mazer limit, the photon emission probability $P_{\text{emission}}(n)$ in the presence of n cavity photons displays resonances at

$$\kappa L = \frac{\sqrt{m(m+1)}}{\sqrt[4]{N}}. \tag{C16}$$

Again, the integer numbers (N,m) label the different resonances.

We perform a similar expansion around the resonances as for the mesa function, use the ansatz

$$\kappa L = \frac{\sqrt{m(m+1)}}{\sqrt[4]{N}} + d\frac{k}{\kappa}, \tag{C17}$$

and find, taking the limit $k/\kappa \to 0$, the expressions

$$\rho_n^+ = -1,$$

$$\rho_n^- = \begin{cases} \dfrac{i2\sqrt{n+1}d}{(2m+1) - i2\sqrt{n+1}d} & \text{for } n = n_{\text{res}} \\ -1 & \text{otherwise} \end{cases} \tag{C18}$$

for the reflection coefficients and

$$\tau_n^+ = 0,$$

$$\tau_n^- = \begin{cases} \dfrac{(-1)^M(2m+1)}{(2m+1) - i2\sqrt{n+1}d} & \text{for } n = n_{\text{res}} \\ 0 & \text{otherwise} \end{cases} \tag{C19}$$

for the transmission coefficients. The integer n_{res} is defined by

$$n_{\text{res}} = N\left(\frac{M(M+1)}{m(m+1)} \right)^2 - 1, \tag{C20}$$

which is the analog of Eq. (C14).

When we use these expressions, the emission probability in the neighborhood of the (N,m) resonance reduces to

$$P_{\text{emission}}(n) = \begin{cases} \frac{1}{2}\dfrac{(2m+1)^2}{(2m+1)^2 + 4(n+1)d^2} & \text{if } n = n_{\text{res}} \\ 0 & \text{otherwise.} \end{cases} \tag{C21}$$

[1] M. O. Scully, G. M. Meyer, and H. Walther, Phys. Rev. Lett. **76**, 4144 (1996).
[2] G. M. Meyer, M. O. Scully, and H. Walther, Phys. Rev. A **56**, 4142 (1997).
[3] The first realization of a micromaser was reported in D. Meschede, H. Walther, and G. Müller, Phys. Rev. Lett. **54**, 551 (1985).
[4] P. Filipowicz, J. Javanainen, and P. Meystre, Phys. Rev. A **34**, 3077 (1986).
[5] See, for example, D. Park, *Introduction to the Quantum Theory* (McGraw-Hill, New York, 1992).
[6] P. F. Byrd and M. D. Friedman, *Handbook of Elliptic Integrals for Engineers and Physicists* (Springer, Berlin, 1954).
[7] B.-G. Englert, J. Schwinger, and M. O. Scully, in *New Frontiers in Quantum Electrodynamics and Quantum Optics*, edited by A. O. Barut (Plenum, New York, 1990), p. 513.
[8] Laser-cooling techniques are reviewed in *Laser Manipulation of Atoms and Ions*, edited by E. Arimondo, W. D. Phillips, and F. Strumia (North-Holland, Amsterdam, 1992).
[9] B.-G. Englert, J. Schwinger, A. O. Barut, and M. O. Scully, Europhys. Lett. **14**, 25 (1991).
[10] W. W. Hansen and R. D. Richtmyer, J. Appl. Phys. **10**, 189 (1939).
[11] F. E. Terman, *Radio Engineers' Handbook* (McGraw-Hill, New York, 1943).
[12] H. Meinke and F. W. Gundlach, *Taschenbuch der Hochfrequenztechnik*, 3rd ed. (Springer, Berlin, 1968).
[13] We assume the holes to be small.
[14] S. Flügge, *Rechenmethoden der Quantentheorie* (Springer, Berlin, 1993).
[15] I. S. Gradshteyn and I. M. Ryzhik, *Table of Integrals, Series, and Products* (Academic, Boston, 1994).